On the relationship between fabric and hydraulic conductivity of Enhanced Bentonites

Proceedings of the 9ICEG
9th International Congress on Environmental Geotechnics
25-28 June, 2023 | Chania, Greece

https://doi.org/10.53243/ICEG2023-81

On the relationship between fabric and hydraulic conductivity of Enhanced Bentonites

N. Guarena[1], A. Dominijanni[2] and M. Manassero[3]

[1]*Research Associate, Polytechnic University of Turin, Turin, Italy, email: nicolo.guarena@polito.it*

[2]*Associate Professor, Polytechnic University of Turin, Turin, Italy, email: andrea.dominijanni@polito.it*

[3]*Full Professor, Polytechnic University of Turin, Turin, Italy, email: mario.manassero@polito.it*

ABSTRACT

Available experimental evidence on the permeability of enhanced bentonites, which comprise natural smectitic clays amended with polymers or organic compounds, has been critically interpreted through a theoretical framework based on the use of a modified form of the Kozeny-Carman equation, to relate the measured hydraulic conductivity to the clay fabric. Based on this interpretation, the average number of lamellae per tactoid, $N_{l,AV}$, which reflects the clay fabric via the separation of the pore space between conductive and non-accessible interlayer pores, has been determined for four enhanced bentonites, viz., Multiswellable Bentonites (MSBs), Dense Prehydrated GCLs (DPH-GCLs), HYPER Clays (HCs), and Bentonite Polymer Composites (BPCs). The variation in the so determined $N_{l,AV}$ values due to a change in the ionic strength of the permeant solution has then been characterised. While intergranular pore clogging by sodium polyacrylate has been shown to be the primary factor controlling the conductive porosity of BPC upon exposure to concentrated electrolyte solutions, preservation of a dispersed clay fabric via intercalation of sodium carboxymethyl cellulose (Na-CMC) between the montmorillonite unit layers has been shown to affect the behaviour of DPH-GCLs. As with BPC, the calculated values of $N_{l,AV}$ for MSB have consistently been found to be greater than the expected values for natural (unamended) bentonites. However, in the case of MSBs, the decrease in the conductive porosity can be ascribed to the greater compressibility of the solid skeleton, which results from mixing with propylene carbonate.

Keywords: aggressive leachates, bentonite fabric, chemical compatibility, geosynthetic clay liners, hydraulic conductivity, polymer amendments

1 INTRODUCTION

Bentonite-based barriers are increasingly being accepted as replacements for traditional pollutant containment systems over a wide range of geoenvironmental applications, due to their low hydraulic conductivity, k, upon permeation with low ionic strength aqueous solutions (Puma et al., 2015), their ability to accommodate large differential settlements without cracking, their self-healing when subjected to punctures during handling and installation, and their ability to exhibit semipermeable membrane behaviour (Guarena et al., 2022). The unique physico-chemical properties of bentonite clays have been shown to be beneficial for the long-term containment performance of bentonite-based barriers, provided the permeant solution is sufficiently dilute and the bentonite exchange complex is dominated by monovalent cations (e.g. Na^+ or K^+). However, substitution of multivalent cations (e.g. Ca^{2+} or Mg^{2+}) for monovalent cations, which can occur after prolonged exposure to contaminated liquids that have a low monovalent-to-multivalent cation ratio, suppresses the osmotic swelling potential and can lead to an increase in hydraulic conductivity over a range of one to several orders of magnitude (Shackelford et al., 2000). The adverse effect on hydraulic conductivity caused by the interaction with liquids with aggressive chemistries, such as hypersaline solutions in brine evaporation ponds, acidic leachates in mine tailing impoundments, and alkaline leachates resulting from aluminium refining operations, has stimulated research on the development of chemically modified bentonites, referred to herein as Enhanced Bentonites (EBs) that comprise natural bentonites (NBs) amended with organic compounds or polymers for increased resistance to hydraulic incompatibility upon exposure to aggressive liquids.

The most relevant EBs for environmental lining applications can be subdivided into two broad categories on the basis of the type of enhancement chemicals. The first category includes EBs that are obtained by polymerising an organic monomer dissolved in a bentonite slurry or by directly mixing air-dried bentonite with a polymeric solution, leading to a variety of commercial products such as Bentonite Polymer Composites (BPCs) (Scalia, 2012), Dense Prehydrated GCLs (DPH-GCLs) (Flynn & Carter, 1998), and HYPER Clays (HCs) (Di Emidio, 2010). All of these polymer-amended bentonites are blended with anionic (negatively charged) polymers, namely sodium polyacrylate (Na-PAA) in the case of BPCs and sodium carboxymethyl cellulose (Na-CMC) in the case of DPH-GCLs and HCs. The second category includes EBs that are treated with organic solvents which have large dielectric constants and dipole moments (Kondo, 1996), such as Multiswellable Bentonites (MSBs) that are bentonites enhanced with propylene carbonate (PC). Although the literature abounds with experimental studies devoted to assessing the impact of chemical modifications on the hydraulic conductivity of EBs upon contact with single-salt aqueous solutions, natural seawater, and synthetic leachates, the understanding of the pore-scale mechanisms that are responsible for the improved hydraulic containment performance of EBs relative to unenhanced NBs is still in development.

On the basis of a comprehensive review on the available experimental evidence pertaining to the hydraulic, diffusive, and membrane behaviour of EBs, Scalia et al. (2018) grouped the mechanisms believed to underlie the increased hydraulic compatibility of EBs into three categories, namely (1) enhanced osmotic swelling, (2) intergranular pore clogging, and (3) prevention of cation exchange. While the protection of chemically modified bentonites from multivalent for monovalent cation exchange is not supported by the existing evidence, additional osmotic swelling has been postulated by most researchers to occur in the case of MSBs. In fact, the intercalation of the organic molecules (e.g. PC) between the finest fabric units of bentonites has been shown to induce an increase in the basal spacing of the clay minerals (Onikata et al., 1999; Fehervari et al., 2016a; Gates et al., 2016) which, in turn, is regarded as the reason for the improved hydraulic resistance. Although Kolstad et al. (2004) and Di Emidio et al. (2015) postulated that DPH-GCLs and HCs similarly benefit from the enhancement of osmotic swelling, Scalia et al. (2018) argued that the poor correlation between swell index (SI) and k observed for BPCs and HCs suggests that the flow paths become narrower and more tortuous independent of swelling, likely due to partial clogging of the conductive pores by water soluble polymers, whereas the physical preconditioning of DPH-GCLs (i.e. prehydration and densification) may be the reason for the poor correlation between SI and k of DPH-GCLs.

The objective of this paper is to further elucidate the microscale phenomena that affect the macroscopically measured hydraulic conductivity of EBs under fully saturated conditions. This objective is achieved through an original interpretation of the results of the permeability tests published in the literature. This interpretation relies on the use of a modified form of the Kozeny-Carman equation that allows the k measurements to be related to the bentonite fabric, which is unequivocally defined through a single state parameter referred to herein as the average number of lamellae per tactoid, $N_{l,AV}$.

2 BENTONITE NANO- AND MICRO-PORE STRUCTURES

The term “bentonite” commonly refers to clay soils with a high content (e.g. > 70% by weight) of montmorillonite (Egloffstein, 2001), a planar 2:1 type phyllosilicate that belongs to the smectite group, whose basic structural unit is approximately 0.96 nm thick and is characterised by a surplus of negative electric charge. The existence of this permanent surface charge is responsible for the sensitivity of the bentonite fabric to the chemical composition of the permeant solution, as a variation in the concentration and valence (charge) of the dissolved ionic species can induce a spatial rearrangement of the montmorillonite unit layers, also referred to as lamellae or platelets, which, in turn, causes a change in the size and in the distribution of the bentonite pores (Dominijanni et al., 2019). Thus, any assessment of the containment performance of bentonite-based barriers should consider the macro-scale impact of the soil fabric modifications, which are mainly controlled by the permeant chemistry, the sequence of exposure to the permeant solutions, and the soil porosity.

The fabric of montmorillonite-rich clay soils comprises tactoids or quasicrystals, wherein from two to several thousands of montmorillonite lamellae are stacked in a nearly parallel array, thus giving rise to nm-sized interlayer pores and μm-sized intertactoid pores (Hueckel et al., 2002). Because of the reduced void volume delimited by adjacent lamellae within the tactoids, water molecules and ionic species that enter the interlayer pores are bound tightly to the mineral surface and, hence, are

characterised by an extremely low mobility, whereas the solvent and solutes migrate relatively unimpeded in the larger intertactoid pores.

In addition to the aforementioned differences in the transport properties, the mechanisms that control the volume change behaviour of the interlayer and intertactoid pores also differ (Laird, 2006). The basal spacing, d_{001}, between adjacent lamellae comprising tactoids and, thus, the extent of the so-called crystalline swelling are dictated by the number of discrete monolayers of water molecules that intercalate in the interlayer pore space, which are generally equal to 4 monolayers (d_{001} approximately equal to 19 Å) for the bulk dry densities that are representative of geosynthetic clay liners (GCLs). Crystalline swelling is a process that occurs in the interlayer pore space, and is only weakly influenced by the electrolyte concentration of the equilibrium bulk solution. Although crystalline swelling may play an important role under unsaturated conditions, the volume change behaviour of saturated bentonites is primarily governed by the osmotic phenomenon, which takes place in the intertactoid pore space and is sensitive to the ionic strength of the permeant solution (Musso et al., 2017; Dominijanni et al., 2018).

The dual-porosity model illustrated in Figure 1 and proposed by Manassero (2020), which consists of a parallel alignment of equally spaced tactoids, where a single state parameter, referred to as the average number of montmorillonite lamellae per tactoid, $N_{l,AV}$, is needed to completely describe the soil fabric, is adopted herein. An effective specific surface, S_{eff}, which is associated with the external surface of the tactoids interacting with the mobile portion of the pore solution, can be calculated once the total specific surface, S_{tot}, is known:

$$S_{eff} = \frac{S_{tot}}{N_{l,AV}} \tag{1}$$

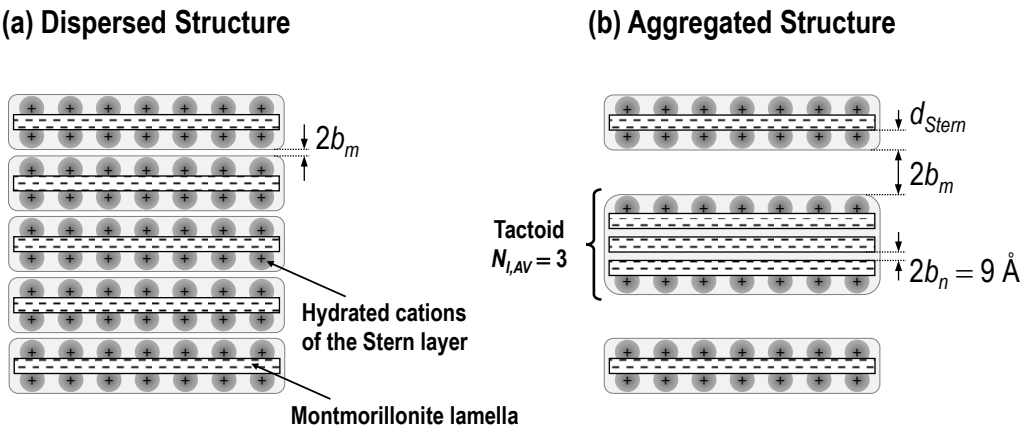

Figure 1. *Schematic view of the bentonite fabric, showing both (a) a dispersed structure of the montmorillonite lamellae and (b) an aggregated structure wherein several lamellae are condensed to form the tactoids (modified from Manassero, 2020).*

The void ratio corresponding to the nonconductive nano-pores, e_n, including both the interlayer porosity and the layer of hydrated cations specifically adsorbed on the mineral surface, commonly referred to as the Stern layer, can be defined as follows:

$$e_n = b_n \rho_{sk} S_{tot} \left(\frac{N_{l,AV} - 1 + d_d}{N_{l,AV}} \right) \tag{2}$$

where b_n is the half distance between the lamellae in the tactoid (b_n = 0.45 nm), ρ_{sk} is the density of the solid phase, and d_d, which can be assumed equal to 4, is the thickness of the Stern layer divided by b_n.

The void ratio corresponding to the conductive micro-pores, e_m, can then be calculated as the difference between the total void ratio, e, and the nano-void ratio ($e_m = e - e_n$). The half distance between the tactoids, b_m, which is also defined as the half width of the conductive micro-channels that have a slit-like geometry, is related to the micro-void ratio according to the following relation:

$$b_m = \frac{e_m}{\rho_{sk} S_{eff}} \tag{3}$$

Although some of the pore-scale mechanisms underlying the bentonite flocculation/dispersion phenomena can be framed, at least from a qualitative viewpoint, in the context of the Derjaguin-Landau-Verwey-Overbeek (DLVO) theory for colloidal particles (Luckham & Rossi, 1999), the development of a mechanistic model that is able to quantify $N_{l,AV}$ as a function of the chemical and mechanical boundary conditions, even in the simplest case of a homogeneous and monomineral clay saturated with an aqueous solution of a single electrolyte, has never been attempted. Despite the lack of a physically sound model, the following phenomenological equation can be used to simulate the effect of the aforementioned pore-scale mechanisms, as proposed by Manassero et al. (2018) and Manassero (2020) in the form of the Fabric Boundary Surface (FBS):

$$N_{l,AV} = N_{l,AV0} + \frac{\alpha}{e_m}\left(\frac{c_s}{c_0} + 1\right) + \beta e_m \left[1 - \exp\left(-\frac{c_s}{c_0}\right)\right] \tag{4}$$

where c_s is the equivalent concentration of the electrolyte, which is hypothesised to be completely dissociated into the constituent ions, c_0 is the reference equivalent concentration (1 eq/L), and $N_{l,AV0}$ (≥ 1), α (≥ 0), and β (≥ 0) are dimensionless parameters, which allow the microstructural arrangement of a given bentonite to be assessed while varying the electrolyte concentration of the equilibrium bulk solution and the total void ratio.

Based on Equation (4), the bentonite flocculation that is induced by an increase in the ionic strength of the pore solution is favoured by high values of the micro-void ratio, due to the weaker constraint to the random thermal (Brownian) motion and the greater likelihood of the tactoids approaching each other until their mutual attractive forces become dominant. Nevertheless, compaction at a high bulk dry density (i.e. low micro-void ratio) also favours aggregation of the tactoids, which are forced to be so close that they eventually yield to their mutual attractive forces, regardless of the magnitude of the electrostatic repulsive forces, with the chemical composition of the pore solution playing a subordinate role compared to compaction. Therefore, the aggregation state of bentonites can be interpreted as controlled by these two flocculation mechanisms, the former of which is driven by a chemical action and prevails at low-to-medium densities, whereas the latter is driven by a mechanical action and prevails at high densities.

Calibration of the FBS parameters was first attempted by Manassero (2020), on the basis of the experimental results provided by Petrov & Rowe (1997), who conducted a series of hydraulic conductivity tests on conventional needle-punched GCL specimens hydrated with distilled water (specimens subjected to both prehydration and posthydration confinement were considered) and subsequently permeated with sodium chloride (NaCl) solutions with concentrations in the 0.01 to 2.0 M range. Interpretation of the Petrov & Rowe (1997) test results yielded a set of c_s, e_m, and $N_{l,AV}$ data that were fitted according to Equation (4), thus allowing the FBS parameters of the prehydrated needle-punched GCL to be obtained ($N_{l,AV0}$ = 1.56; α = 8.82; β = 10.01).

3 PORE-SCALE INTERACTION MECHANISMS IN ENHANCED BENTONITES

3.1 Modelling the saturated flow through bentonites

Among various indirect methods to evaluate the pore structure of fully-saturated bentonites, interpretation of permeability test results has been recognised as suitable to investigate flocculation/dispersion phenomena over a wide range of soil porosities and salt concentrations of the permeant solution, since the hydraulic conductivity can vary over several orders of magnitude as a result of a variation in the bentonite fabric (Guarena et al., 2020; Manassero, 2020). Such an interpretation requires a relationship between the hydraulic conductivity and a given number of intrinsic and state parameters based on the principles that underlie the motion of fluids in porous media (Bear, 1972).

Under the assumption that the effect of the streaming potential is negligible, integration of the Navier-Stokes equation for the dual-porosity structural model proposed by Manassero (2020), which consists of a bundle of narrow capillary fissures of constant width, $2b_m$, yields the following modified form of the Kozeny-Carman equation:

$$k = \tau_m n \frac{\gamma_w}{3\mu_w} \frac{e_m^2}{\left(\rho_{sk} S_{eff}\right)^2} \tag{5}$$

where n is the total porosity, γ_w is the water unit weight (γ_w = 9.81 kN/m^3), μ_w is the dynamic viscosity of water (μ_w = 10^{-3} Pa·s), and τ_m is the matrix tortuosity factor, which accounts for the tortuous nature of the conductive pores and can be assessed through the following empirically-based relation (Guarena, 2021):

$$\tau_m = \frac{\chi}{n} \exp(\lambda n) \tag{6}$$

where the first set of model parameters, given as χ = 0.0006088 and λ = 6.7049, is representative of the behaviour of both NBs and EBs, with the exception of BPCs, whereas the second set of model parameters, given as χ = 0.0002473 and λ = 6.8859, only pertains to BPCs.

3.2 Interpretation of the results of permeability tests on Enhanced Bentonites

The long-term hydraulic conductivity tests with single-salt permeant solutions performed by Katsumi et al. (2008) for MSB and DPH-GCL specimens, Kolstad et al. (2004) and Malusis & Daniyarov (2016) for DPH-GCL specimens, Di Emidio et al. (2015) for an HC specimen, and Scalia et al. (2014) for BPC specimens have all been interpreted herein to gain insight into the microstructural arrangement of these EBs, thus leading to the values of $N_{l,AV}$ listed in Table 1. Note that the DPH-GCL specimens tested by Malusis & Daniyarov (2016) and the HC specimen tested by Di Emidio et al. (2015) were subjected to simultaneous measurements of the osmotic and diffusion properties and, hence, the corresponding values of τ_m that were used in Equation (5) have been assumed equal to the values calibrated from the interpretation of the measured reflection or membrane efficiency coefficient and the osmotic effective diffusion coefficient (Guarena, 2021).

In addition to the aforementioned studies, the hydraulic conductivity values that were measured by Norris et al. (2022) on specimens of an EB-GCL, modified through wet mixing with sodium carboxymethyl cellulose of low viscosity (CMCLV) and high viscosity (CMCHV), have been considered, in an attempt to cover the current paucity of data on HCs. Considering the analogies in the treatment procedures of the HC specimen tested by Di Emidio et al. (2015) and the CMC amended EB-GCL specimens tested by Norris et al. (2022), both of these EBs are expected to show a similar type of behaviour, even though the aforementioned treatment procedures are not exactly identical, for instance, in terms of the polymer dosage (2% vs 5% by dry weight), the mixing time of the slurry of bentonite, polymer, and water (30 min vs 10 min), and the grain-size distribution after oven-drying, grinding, and sieving.

In Figure 2, the $N_{l,AV}$ values resulting from the interpretation of the k measurements on EBs are shown versus the micro-void ratio, and also compared with the corresponding iso-concentration curves of the FBS for prehydrated conventional GCLs. The scope of this comparison is to investigate the differences that exist between the aggregation states of NBs hydrated with distilled water, the behaviour of which is assumed to be comparable with that of the GCL tested by Petrov & Rowe (1997), and the considered EBs, in equilibrium with both the diluted and concentrated electrolyte solutions used to simulate aggressive leachates. Thus, an assessment of the impact of the chemical amendment on the sensitivity of the bentonite fabric to the salt concentration of the permeant solution and to the bentonite porosity is possible.

As shown in Figure 2a and aside from the data referring to permeation with deionised water, all the calculated values of $N_{l,AV}$ for the non-prehydrated MSB specimens tested by Katsumi et al. (2008) are consistently greater than the model predictions for prehydrated NBs. The observed increase in $N_{l,AV}$ under the same chemical composition of the permeant solution can be ascribed, in part, to the absence of exposure to deionised water prior to permeation with the testing solutions (Shackelford et al., 2000). However, the decrease in the measured k for the MSB specimens subjected to intermediate NaCl concentrations (200 ≤ c_s ≤ 1000 meq/L) relative to the results of comparative permeability tests carried out by Katsumi et al. (2008) on unamended (non-prehydrated) bentonite specimens should be interpreted in view of the modification of the bentonite swelling behaviour, which is due to mixing with liquid PC. Even though the effectiveness of PC in promoting crystalline swelling has been corroborated

by an extensive experimental evidence, including Fourier transform infrared absorption spectra and X-ray diffraction patterns recorded on powdered PC-montmorillonite complexes (Onikata et al., 1999; Mazzieri et al., 2010; Fehervari et al., 2016a), the results of the swell index tests performed by Katsumi et al. (2008), Mazzieri et al. (2010), and Fehervari et al. (2016b) did not indicate any overall significant improvement in the ability of MSBs to undergo osmotic swelling relative to NBs. Also, in some cases, evidence of a greater compressibility of the solid skeleton, which must occur at the expense of a reduction in the intertactoid porosity, was obtained for MSBs. Such evidence is further confirmed by the greater volumetric compressive strain that was experienced by the MSB specimens tested by Katsumi et al. (2008), which were consolidated up to an average total void ratio of 0.963 for the NaCl concentrations in the 200 to 1000 meq/L range. Upon completion of consolidation, the MSB specimens were characterised by an appreciably lower total void ratio than the values ($1.971 \leq e \leq 3.046$) associated with the unamended bentonite specimens subjected to comparative permeability tests, under the same effective confining stress and the same chemical composition of the permeant solution. According to Equation (5), the greater compressibility of the solid skeleton, which is reflected by the low values of the micro-void ratio shown in Figure 2a, can be regarded as the reason for the observed decrease in k.

Table 1. *Range of intrinsic, state, and fabric parameters of the EB specimens subjected to permeability tests by Katsumi et al. (2008), Kolstad et al. (2004), Malusis & Daniyarov (2016), Di Emidio et al. (2015), Norris et al. (2022), and Scalia et al. (2014).*

	Specimen type	Salt	CEC [(a)]	ρ_{sk}	e	c_s	k	$N_{l,AV}$
			(meq/100 g)	(Mg/m^3)	(-)	(meq/L)	(m/s)	(-)
Katsumi et al. (2008)	MSB	NaCl	82.0	2.478	0.905	0	$7.03 \cdot 10^{-12}$	8.87
		$CaCl_2$			2.407	2000	$2.64 \cdot 10^{-9}$	236.7
	DPH-GCL	$CaCl_2$	104.0	2.73	2.249	500	$1.17 \cdot 10^{-12}$	5.11
					2.782	2000	$3.63 \cdot 10^{-12}$	9.49
Kolstad et al. (2004)	DPH-GCL	NaCl	84.1 [(b)]	2.5	1.2	0	$3.7 \cdot 10^{-12}$	36.92
		$CaCl_2$				2000	$4.2 \cdot 10^{-12}$	38.94
Malusis & Daniyarov (2016)	DPH-GCL	KCl	52	2.69	1.128	0	$7.0 \cdot 10^{-13}$	4.26
					1.778	160	$2.0 \cdot 10^{-12}$	11.67
Di Emidio et al. (2015)	HYPER Clay 2%	$CaCl_2$	47.29	2.53	2.546	0	$5.3 \cdot 10^{-12}$	2.62
						10	$6.5 \cdot 10^{-12}$	2.83
Norris et al. (2022)	CMCLV EB-GCL	NaCl	78.0	2.76	2.429	334	$6.7 \cdot 10^{-11}$	15.05
		$CaCl_2$			2.843	500	$4.1 \cdot 10^{-10}$	49.35
	CMCHV EB-GCL	NaCl	78.0	2.76	2.926	334	$2.3 \cdot 10^{-11}$	7.19
		$CaCl_2$			3.257	500	$3.8 \cdot 10^{-10}$	32.25
Scalia et al. (2014)	BPC	$CaCl_2$	85.5	2.71	1.6	0	$1.8 \cdot 10^{-11}$	1.15
					13.5	400	$8.1 \cdot 10^{-11}$	90.12

[(a)] As discussed by Shang et al. (1994), the cation exchange capacity, CEC, can be related to S_{tot} according to the CEC = σS_{tot}/F relation, where σ is the surface charge density of montmorillonite (0.114 C/m^2) and F is Faraday's constant ($9.6485 \cdot 10^4$ C/mol).
[(b)] The CEC value of the DPH-GCL specimens tested by Kolstad et al. (2004) has been estimated from the smectite content (89%), which was determined by means of XRD.

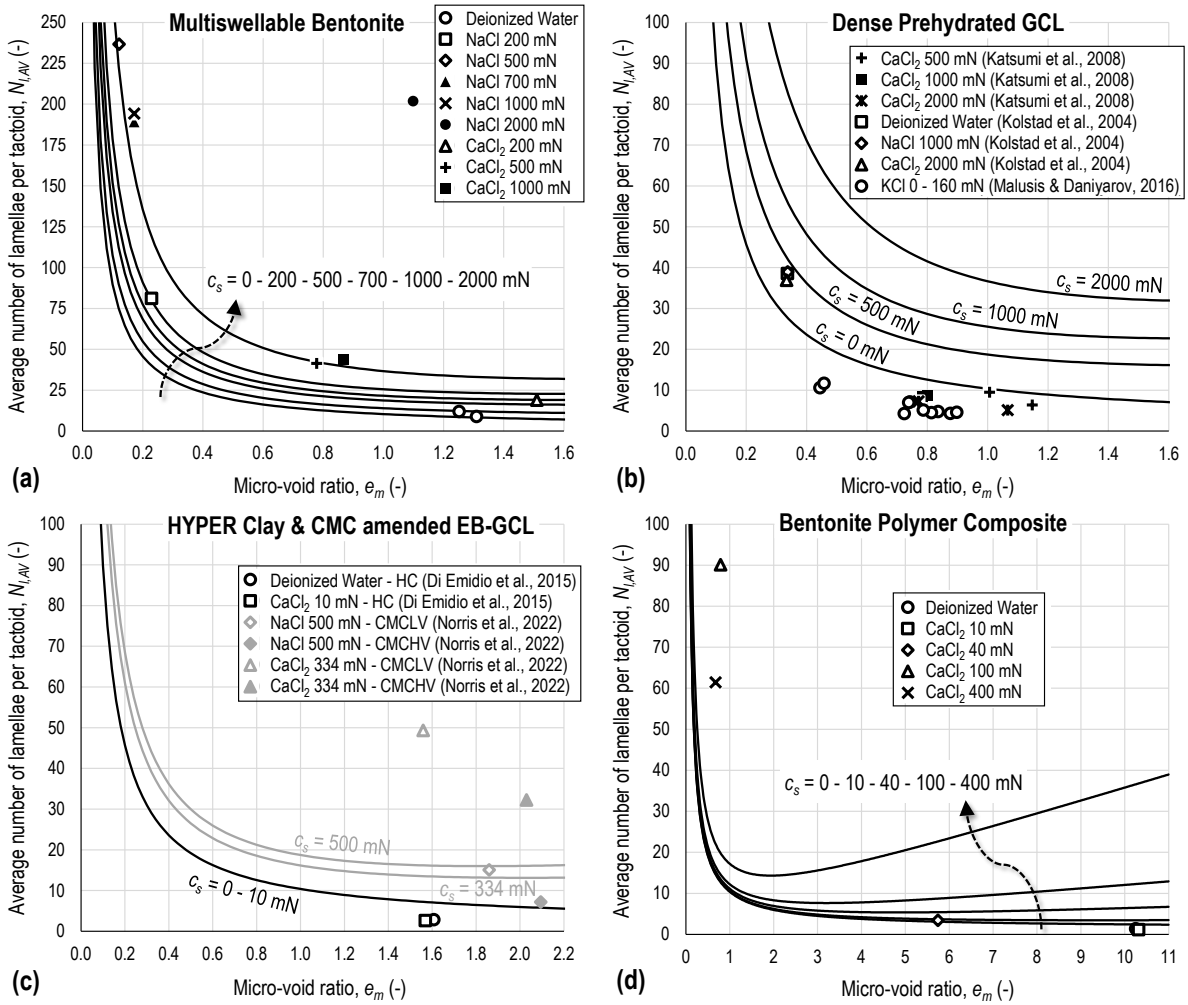

Figure 2. *Comparison between the iso-concentration curves of the FBS (continuous lines), calibrated on the hydraulic conductivity test results of Petrov & Rowe (1997), and the values of the average number of lamellae per tactoid, $N_{l,AV}$, obtained from interpretation of the measured hydraulic conductivity of: (a) the MSB tested by Katsumi et al. (2008); (b) the DPH-GCL tested by Katsumi et al. (2008), Kolstad et al. (2004), and Malusis & Daniyarov (2016); (c) the HC tested by Di Emidio et al. (2015) and the CMC amended EB-GCL tested by Norris et al. (2022); (d) the BPC tested by Scalia et al. (2014).*

Unlike MSBs, the ability of DPH-GCLs to maintain a dispersed bentonite fabric and, hence, an extremely low hydraulic conductivity ($k \sim 10^{-12}$ m/s) upon permeation with concentrated calcium chloride ($CaCl_2$) solutions is reflected by the values of $N_{l,AV}$ that lie close to the iso-concentration curve for deionised water (Figure 2b). This behaviour can be attributed to the treatment procedure developed for DPH-GCLs, which involves prehydration of the dry sodium bentonite with an aqueous solution containing Na-CMC, followed by preconsolidation (densification) through vacuum extrusion. The results of X-ray diffraction tests by Qiu & Yu (2008), Mazzieri & Di Emidio (2015), and Mazzieri & Bernardo (2022) provide evidence of the intercalation of Na-CMC within the interlayer pore space and a higher degree of dispersion of the bentonite fabric after blending with the anionic polymer, whereas scanning electron micrographs (SEMs) by Mazzieri & Bernardo (2022) suggest that the highly oriented and densely packed structure of dispersed montmorillonite lamellae, resulting from prehydration and densification, is preserved after permeation with aggressive leachates. Therefore, inhibition of the flocculation mechanism related to the increase in the ionic strength of the pore solution can be attributed to the treatment procedure. The observed agreement between the calculated values of $N_{l,AV}$ and the iso-concentration curve for deionised water at the lowest e_m also indicates that the same treatment procedure is not effective in hindering aggregation when DPH-GCLs are consolidated under a high effective confining stress, since the flocculation mechanism related to compaction is not affected by the polymer intercalation between the montmorillonite lamellae.

Low k values also were evident for the HC specimen, consistently with the low calculated values of $N_{l,AV}$ (Figure 2c). However, the salt solutions used by Di Emidio et al. (2015) for HC were not sufficiently concentrated to allow for an assessment of the influence of Na-CMC on the aggregation state of the modified bentonite upon exposure to harsh chemical environments. Although the preparation of HC involves a similar polymeric solution to that used for DPH-GCLs, the slurry of bentonite, polymer, and water is oven-dried at 105 °C instead of being vacuum-extruded and, as such, the potential contribution of densification to the long-term barrier performance is excluded. The results of the permeability tests performed by Norris et al. (2022) on non-prehydrated CMC amended EB-GCL specimens have been interpreted with the aim of addressing this latter issue, and the corresponding $N_{l,AV}$ values are reported in grey in Figure 2c. These results suggest that the polymer viscosity plays a relevant role in determining the bentonite fabric, with the high viscosity Na-CMC being more effective in favouring a dispersed and highly porous microstructure than the low viscosity Na-CMC. Furthermore, the possibility of maintaining a dispersed fabric upon permeation with high ionic strength aqueous solutions depends to a great extent on the electrochemical charge of the cationic species that result from the salt dissociation. In the case of a prevalence of monovalent cations (e.g. Na^+), blending with Na-CMC may be associated with values of $N_{l,AV}$ that are lower than or comparable with the model predictions for prehydrated NBs, whereas the presence of divalent cations is observed to be detrimental to the ability of Na-CMC to prevent the bentonite from flocculating at high salt concentrations. On the basis of such evidence, the contribution of densification to the long-term barrier performance may not be of secondary importance, particularly when low viscosity Na-CMC is used and multivalent cations are contained in the permeant solution. However, further research is needed on HC, prepared according to the treatment procedure described by Di Emidio et al. (2015), to verify this conclusion.

The relatively high values of $N_{l,AV}$ that can be observed for the nonprehydrated BPC specimens tested at the highest $CaCl_2$ concentrations (Figure 2d) can be attributed, in a similar way to the MSB specimens, to direct permeation with the chemical solutions, i.e., without prehydration. Given that Na-PAA, a cross-linked polymer hydrogel that is able to absorb large amounts of water, does not prevent aggregation of the bentonite microstructure upon contact with concentrated electrolyte solutions, the reduction in hydraulic conductivity noted by Scalia et al. (2014), relative to the results of comparative permeability tests carried out on unamended (non-prehydrated) bentonite specimens, should be correlated with the low values of τ_m that result from Equation (6) and the low values of e_m observed in Figure 2d. However, unlike MSBs, the decrease in the pore volume accessible to the liquid flow with increasing $CaCl_2$ concentration is caused by the polymer hydrogel that partially occludes the bentonite pores, with this latter mechanism being corroborated in a number of published studies. Such evidence includes X-ray diffraction patterns recorded on NB and BPC specimens (Scalia, 2012; Scalia & Benson, 2017), which are indicative of the absence of intercalation of the long-chain macromolecules of Na-PAA between the montmorillonite lamellae, and pore-scale images of EB-GCL specimens containing anionic polyacrylamide (Tian et al., 2019), wherein the polymer hydrogel is shown to form a separate phase that fills the intertactoid pore volume. For the sake of comparison, no evidence of polymer strands or web binding to the tactoids is apparent in the SEMs obtained by Mazzieri & Bernardo (2022), thus reinforcing the hypothesis that the mechanism governing the hydraulic and chemical transport behaviour of BPCs (i.e. partial clogging of the conductive pores) is substantially different from that of DPH-GCLs (i.e. enhanced dispersion of the bentonite fabric, due to intercalation of Na-CMC within the interlayer pore space and densification through vacuum extrusion).

4 CONCLUSIONS

The available literature pertaining to the laboratory assessment of the hydraulic conductivity, k, of Enhanced Bentonites (EBs) has been interpreted via a theoretical model that allows the k measured at the macroscale to be related to a single state parameter, which represents the bentonite fabric and is referred to as the average number of lamellae per tactoid, $N_{l,AV}$. The study has focused on four EBs, viz., Multiswellable Bentonites (MSBs), Dense Prehydrated GCLs (DPH-GCLs), HYPER Clays (HCs), and Bentonite Polymer Composites (BPCs), with the objective of further elucidating the interaction mechanisms between the bentonite phase and the chemical additives.

Enhanced osmotic swelling, which was indicated by Scalia et al. (2018) as one of the three mechanisms believed to influence the behaviour of EBs, has herein been ruled out as a factor that contributes to improving the sealing ability of MSBs, which instead manifest a greater compressibility than unamended bentonites. The greater volumetric compressive strain experienced by MSBs has to occur at the

expense of a reduction in the intertactoid porosity, which in turn is responsible for the observed decrease in measured *k*. Intergranular pore clogging has been confirmed as the primary mechanism that controls the *k* of BPCs upon permeation with high ionic strength aqueous solutions. DPH-GCLs are characterised by a low *k* upon exposure to concentrated electrolyte solutions as a result of an enhanced dispersion of the bentonite fabric, which is an additional mechanism relative to those described by Scalia et al. (2018). The same ability to maintain a dispersed fabric has not been observed for MSBs and BPCs, which undergo more extensive flocculation than prehydrated natural bentonites when the specimens are directly permeated with the concentrated electrolyte solutions. Although a similar polymeric solution to that of DPH-GCLs is used in the preparation of HCs, additional research is recommended to verify whether the latter modified clay can benefit from the aforementioned mechanism (i.e. preservation of a dispersed bentonite fabric), even in the absence of the preconsolidation effect.

REFERENCES

Bear, J. (1972). Dynamics of fluids in porous media. New York: American Elsevier Publishing Company.

Di Emidio, G. (2010). Hydraulic and chemico-osmotic performance of polymer treated clays. Doctoral dissertation, Ghent University. Ghent, Belgium.

Di Emidio, G., Mazzieri, F., Verastegui-Flores, R.D., Van Impe, W., & Bezuijen, A. (2015). Polymer-treated bentonite clay for chemical-resistant geosynthetic clay liners. Geosynthetics International, 22(1), 125-137.

Dominijanni, A., Guarena, N., & Manassero, M. (2018). Laboratory assessment of semipermeable properties of a natural sodium bentonite. Canadian Geotechnical Journal, 55(11), 1611-1631.

Dominijanni, A., Fratalocchi, E., Guarena, N., Manassero, M., & Mazzieri, F. (2019). Critical issues in the determination of the bentonite cation exchange capacity. Géotechnique Letters, 9(3), 205-210.

Egloffstein, T.A. (2001). Natural bentonites - Influence of the ion exchange and partial desiccation on permeability and self-healing capacity of bentonites used in GCLs. Geotextiles and Geomembranes, 19(7), 427-444.

Fehervari, A., Gates, W.P., Turney, T.W., Patti, A.F., & Bouazza, A. (2016a). Cyclic organic carbonate modification of sodium bentonite for enhanced containment of hyper saline leachates. Applied Clay Science, 134, 2-12.

Fehervari, A., Gates, W.P., Patti, A.F., Turney, T.W., Bouazza, A., & Rowe, R.K. (2016b). Potential hydraulic barrier performance of cyclic organic carbonate modified bentonite complexes against hyper-salinity. Geotextiles and Geomembranes, 44(5), 748-760.

Flynn, B., & Carter, G. (1998). Waterproofing material and method of fabrication thereof (U.S. Patent No. 6,537,676 B1). U.S. Patent and Trademark Office.

Gates, W.P., Shaheen, U., Turney, T.W., & Patti, A.F. (2016). Cyclic carbonate-sodium smectite intercalates. Applied Clay Science, 124-125, 94-101.

Guarena, N. (2021). Relevance of chemical and electrical phenomena to the semipermeable properties of natural and modified bentonites. Doctoral dissertation, Polytechnic University of Turin. Turin, Italy.

Guarena, N., Dominijanni, A., & Manassero, M. (2020). From the design of bottom landfill liner systems to the impact assessment of contaminants on underlying aquifers. Innovative Infrastructure Solutions, 5(1), 2.

Guarena, N., Dominijanni, A., & Manassero, M. (2022). The role of diffusion induced electro-osmosis in the coupling between hydraulic and ionic fluxes through semipermeable clay soils. Soils and Foundations, 62(4), 101177.

Hueckel, T., Loret, B., & Gajo, A. (2002). Expansive clays as two-phase, deformable, reactive continua: Concepts and modeling options. In C. Di Maio, T. Hueckel, & B. Loret (Ed.), Chemo-Mechanical Coupling in Clays: From Nano-scale to Engineering Applications, (pp. 105-120). Maratea, Italy.

Katsumi, T., Ishimori, H., Onikata, M., & Fukagawa, R. (2008). Long-term barrier performance of modified materials against sodium and calcium permeant solutions. Geotextiles and Geomembranes, 26(1), 14-30.

Kolstad, D.C., Benson, C.H., Edil, T.B., & Jo, H.Y. (2004). Hydraulic conductivity of a dense prehydrated GCL permeated with aggressive inorganic solutions. Geosynthetics International, 11(3), 233-241.

Kondo, M. (1996). Method of activation of clay and activated clay (U.S. Patent No. 5,573,583). U.S. Patent and Trademark Office.

Laird, D.A. (2006). Influence of layer charge on swelling of smectites. Applied Clay Science, 34(1-4), 74-87.

Luckham, P.F., & Rossi, S. (1999). The colloidal and rheological properties of bentonite suspensions. Advances in Colloid and Interface Science, 82(1-3), 43-92.

Malusis, M.A., & Daniyarov, A.S. (2016). Membrane efficiency and diffusive tortuosity of a dense prehydrated geosynthetic clay liner. Geotextiles and Geomembranes, 44(5), 719-730.

Manassero, M. (2020). Second ISSMGE R. Kerry Rowe Lecture: On the intrinsic, state, and fabric parameters of active clays for contaminant control. Canadian Geotechnical Journal, 57(3), 311-336.

Manassero, M., Dominijanni, A., & Guarena, N. (2018). Modelling hydro-chemo-mechanical behaviour of active clays through the fabric boundary surface. In W. Wu, & H.S. Yu (Ed.), China-Europe Conference on Geotechnical Engineering, Vol. 2 (pp. 1618-1626). Vienna, Austria.

Mazzieri, F., & Di Emidio, G. (2015). Hydraulic conductivity of a dense prehydrated geosynthetic clay liner. Geosynthetics International, 22(1), 138-148.

Mazzieri, F., & Bernardo, D. (2022). Permeability and solute sorption of unamended and polymer-enhanced geosynthetic clay liners. Environmental Geotechnics, Ahead of Print.

Mazzieri, F., Di Emidio, G., & Van Impe, P.O. (2010). Diffusion of calcium chloride in a modified bentonite: Impact on osmotic efficiency and hydraulic conductivity. Clays and Clay Minerals, 58(3), 351-363.

Musso, G., Cosentini, R.M., Dominijanni, A., Guarena, N., & Manassero, M. (2017). Laboratory characterization of the chemo-hydro-mechanical behaviour of chemically sensitive clays. Rivista Italiana di Geotecnica, 51(3), 22-47.

Norris, A., Aghazamani, N., Scalia, J., & Shackelford, C.D. (2022). Hydraulic performance of geosynthetic clay liners comprising anionic polymer-enhanced bentonites. Journal of Geotechnical and Geoenvironmental Engineering, 148(6), 04022039.

Onikata, M., Kondo, M., Hayashi, N., & Yamanaka, S. (1999). Complex formation of cation-exchanged montmorillonites with propylene carbonate: Osmotic swelling in aqueous electrolyte solutions. Clays and Clay Minerals, 47(5), 672-677.

Petrov, R.J., & Rowe, R.K. (1997). Geosynthetic clay liner (GCL) – chemical compatibility by hydraulic conductivity testing and factors impacting its performance. Canadian Geotechnical Journal, 34(6), 863-885.

Puma, S., Dominijanni, A., Manassero, M., & Zaninetta, L. (2015). The role of physical pretreatments on the hydraulic conductivity of natural sodium bentonites. Geotextiles and Geomembranes, 43(3), 263-271.

Qiu, H., & Yu, J. (2008). Polyacrilate/carboxymethylcellulose modified montmorillonite superabsorbent nanocomposite: preparation and water absorbency. Journal of Applied Polymer Science, 107(1), 118-123.

Scalia, J. (2012). Bentonite-polymer composites for containment applications. Doctoral dissertation, University of Wisconsin-Madison. Madison, Wisconsin (USA).

Scalia, J., & Benson, C.H. (2017). Polymer fouling and hydraulic conductivity of mixtures of sodium bentonite and a bentonite-polymer composite. Journal of Geotechnical and Geoenvironmental Engineering, 143(4), 04016112.

Scalia, J., Benson, C.H., Bohnhoff, G.L., Edil, T.B., & Shackelford, C.D. (2014). Long-term hydraulic conductivity of a bentonite-polymer composite permeated with aggressive inorganic solutions. Journal of Geotechnical and Geoenvironmental Engineering, 140(3), 04013025.

Scalia, J., Bohnhoff, G.L., Shackelford, C.D., Benson, C.H., Sample-Lord, K.M., Malusis, M.A., & Likos, W.J. (2018). Enhanced bentonites for containment of inorganic waste leachates by GCLs. Geosynthetics International, 25(4), 392-411.

Shackelford, C.D., Benson, C.H., Katsumi, T., Edil, T.B., & Lin, L. (2000). Evaluating the hydraulic conductivity of GCLs permeated with nonstandard liquids. Geotextiles and Geomembranes, 18(2-4), 133-161.

Shang, J.Q., Lo, K.Y., & Quigley, R.M. (1994). Quantitative determination of potential distribution in Stern-Gouy double-layer model. Canadian Geotechnical Journal, 31(5), 624-636.

Tian, K., Likos, W.J., & Benson, C.H. (2019). Polymer elution and hydraulic conductivity of bentonite-polymer composite geosynthetic clay liners. Journal of Geotechnical and Geoenvironmental Engineering, 145(10), 04019071.